The importance of stress percolation to ductile deformation and shear localization in rocks

Pamela C. Burnley, Geoscience Department, University of Nevada, Las Vegas
Pamela.Burnley@unlv.edu

Abstract

Percolation theory has been used to describe the behavior of a large number of disordered systems including the passage of fluid through porous materials, the spread of forest fires, and the mechanical behavior of granular materials. By virtue of both variations in elastic and plastic properties between different rock forming minerals as well as the plastic and elastic anisotropy of individual mineral grains, polycrystalline aggregates of minerals are elastically and plastically disordered systems. Using 2D finite element models I have shown that stress transmission in rocks can also be described as a percolation problem and that the modulation of stress states within a rock can in some cases, reach levels comparable to the differential load on the rock. The presence of such modulations in the stress state of a rock has many implications for understanding the rock's physical and chemical responses to stress. Stress percolation has been shown to occur in granular materials (the phenomena is sometimes described as "force chains") and plays in important role in the development of shear localization in these materials. Although it is well known that mechanical heterogeneities can cause shear localization in viscous materials, the popular assumption of a Reuss stress state in polycrystalline rocks has made it difficult to explain the development of ductile shear localization in rocks that do not contain pre-existing weak features. The modulations in stress states created by stress percolation create small regions (yield nuclei) distributed throughout the rock that yield well before the bulk of the rock has reached the yield criterion. Local yielding leads to percolation of yielded regions and shear localization. Whether the shear localization remains cryptic or is observable by virtue of the development of large offsets, is a function of the density and distribution of yield nuclei. The spatial distribution of yield nuclei is a function of the nature of the stress percolation pattern as well as the degree of variation in yield strength of the constituent minerals and their distribution throughout the rock. Taking stress percolation into account helps explain why shear localization occurs during ductile deformation and predicts which rock types are more or less prone to develop large-scale shear localization.

*(more details can be found in Burnley (2013)
DOI: 10.1038/ncomms3117)*

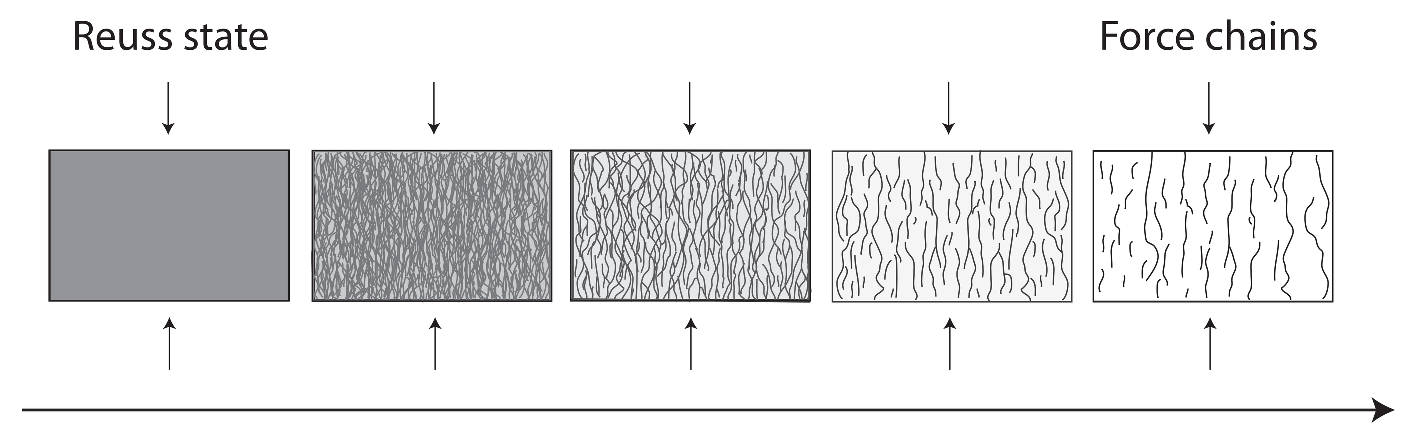

Component Heterogeneity

Percolation

A familiar example:
simulation of oil percolating in sand

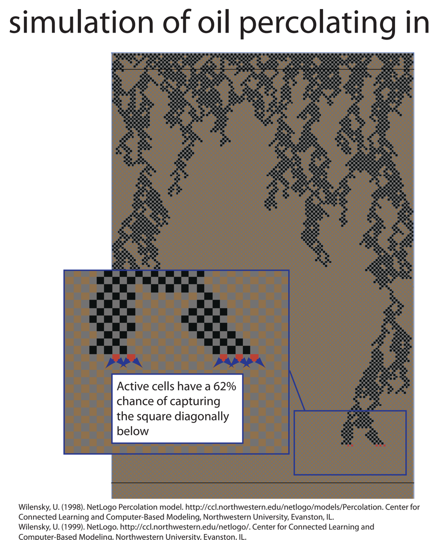

Stress percolation occurs in granular materials

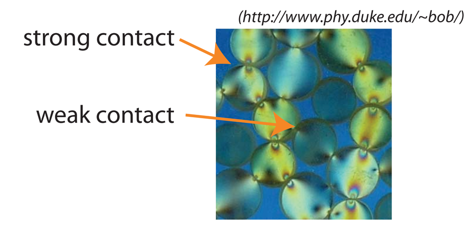

Force chains in photo-elastic disks

Percolation theory is used to describe the behavior of disordered systems

Anisotropy of Single Crystal Elasticity

Elasticity

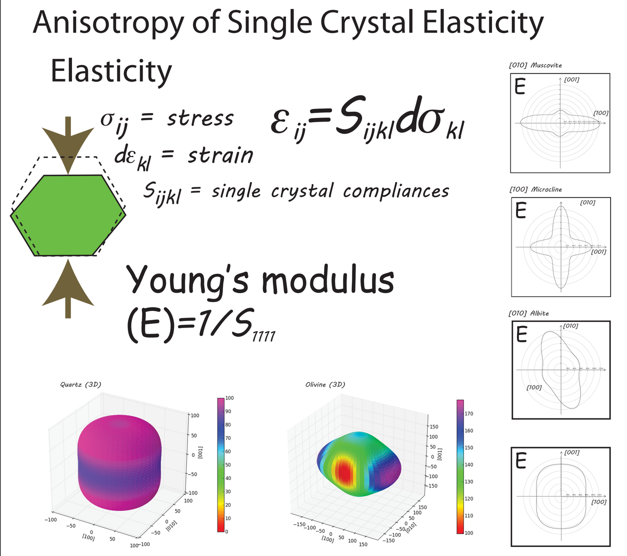

How does the deformation of each crystal add together to create the mechanical response of the aggregate?

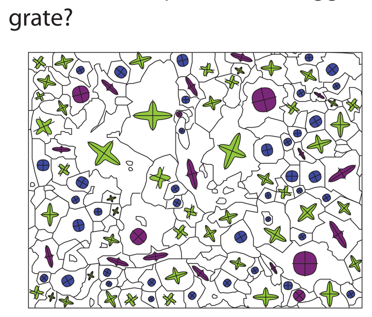

Polycrystals are elastically disordered systems.

The Models

Nodes on the boundaries are shared between structural components. So boundaries have no independent rheology.

Simple hexagons

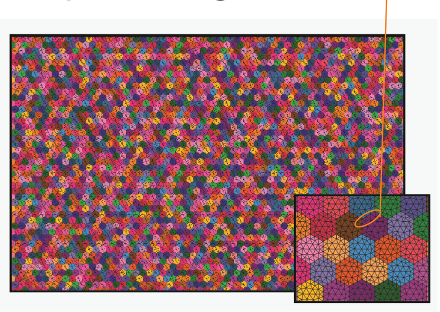

2574 hexagonal "structural components"
48 elements per component
6-noded triangular elements
Grains randomly assigned to 25 subsets
Each subset has E, ν and von Mises yield strength

Rheological properties

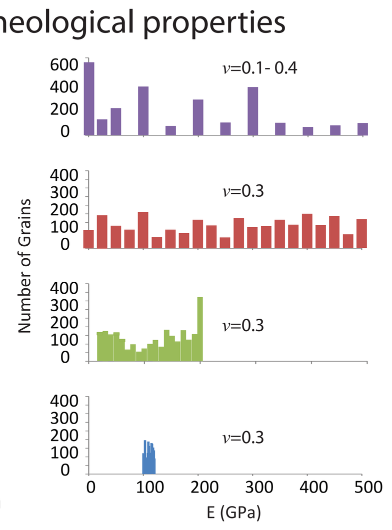

- yeild strength for each material is set to E/100.

"Barre granite"

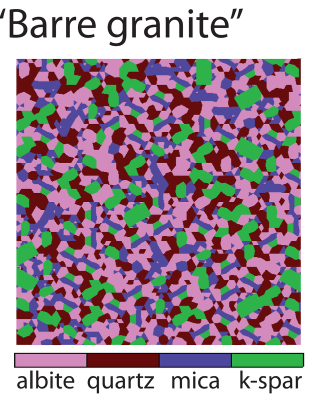

Rheological properties properties

Mineralogy	Area %	Orientations	Yield strength GPa
Albite	35.5%	34	1
K-spar	19.9%	6	1
Quartz	25.4%	20	0.3
Mica	19.3%	7	0.1

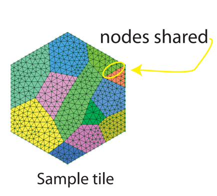

Orientation groups

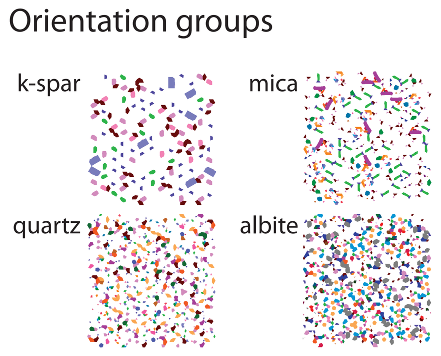

6 tile motifs each with 6 orientations
Tile and tile orientation for each position assigned randomly
6-noded triangular elements
Full elastic tensor description

Boundary conditions

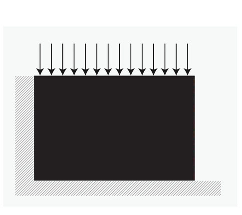

2D plane strain
Top boundary either:
- Fixed displacement
- Constant load
Bottom constrained vertically
Left side constrained horizontally
Right side free

Model Plasticity

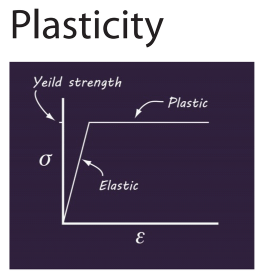

Stress Patterns

Equivalent von Mises stress

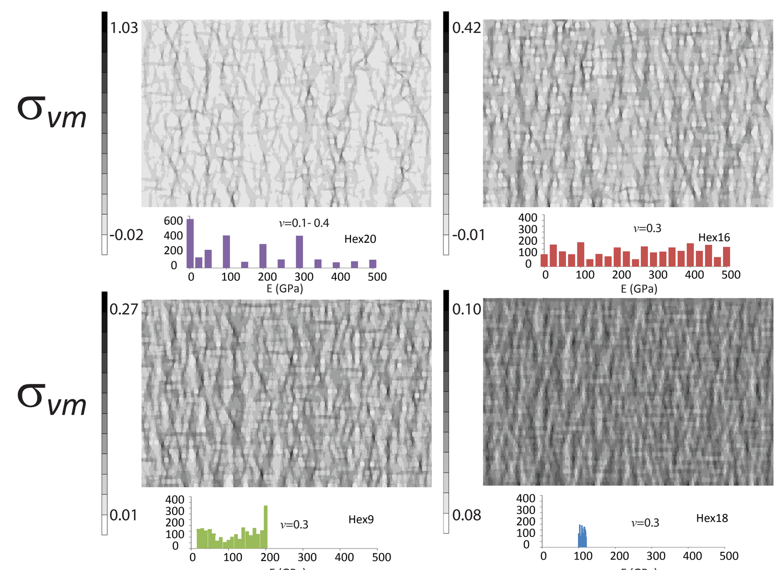

Equivalent von Mises stress patterns reflect patterns in the maximum and minimum compressive stress. All models were loaded with 0.1 GPa along the top edge. The variation in stress states is a function of the heterogeneity and distribution of elastic properties among the grains.

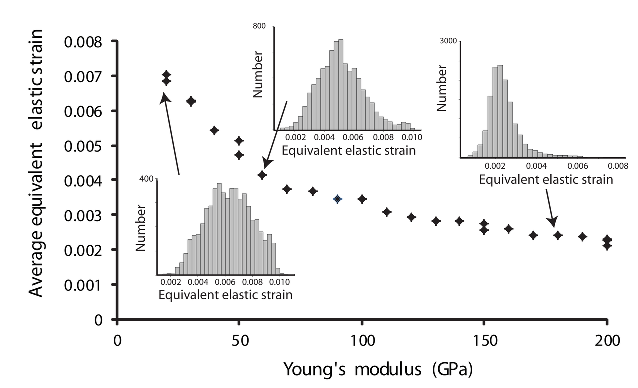

The average elastic strain is inversely proportional to the Young's modulus as is expected. However the distribution of elastic strain within a component population is different from component population to component population. More compliant components show a wider range of elastic states.

Pattern changes accompanying yield

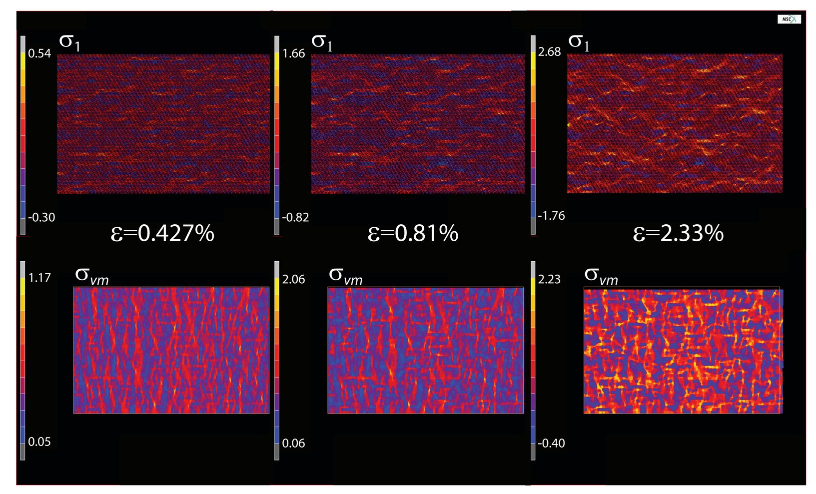

Patterns in σ_1 and equivalent von Mises stress (σ_{vm}) for model hex9 prior to (0.47% strain), during (0.81% strain) and after (2.33 % strain) yielding initiates. This model has no work hardening. The patterns in σ_1 intensify as grains in the model begin to deform plastically which causes the patterns in σ_{vm} to become less coherent.

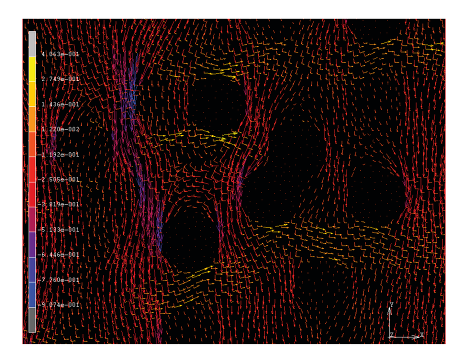

Orientation and magnitude of minimum (σ_3) and maximum (σ_1) components of the stress tensor in a portion of model Hex16. Compression (which is negative), is depicted in orange to blue; tensile stresses are yellow. The arrows point in the direction of the principal components of the tensor.

Stress patterns in "Barre Granite" model

Despite the differences in grain shape and size, the Barre granite model still produces stress percolation patterns. The patterns change as portions of the model begin to yield at higer strain

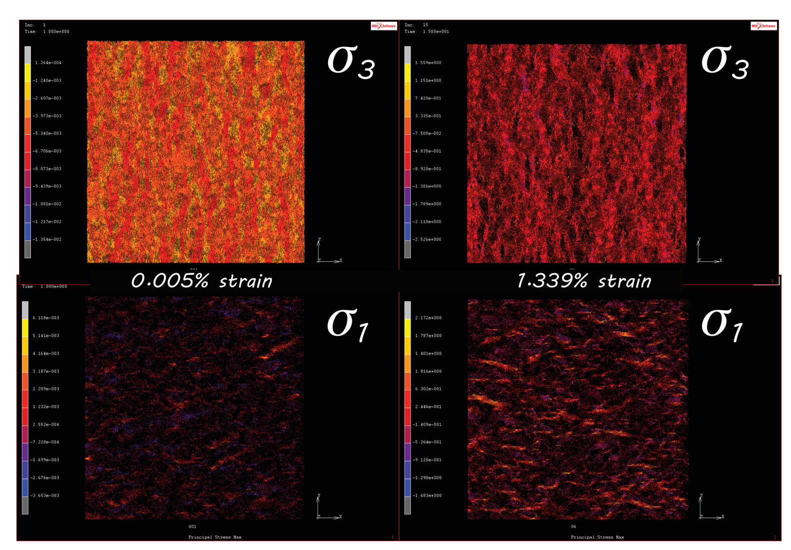

Strain Patterns

All models experience shear localization. Shear localization is not a result of local weakening but results from nucleation of plastic deformation at places with either high stress or low yield

Equivalent von Mises strain

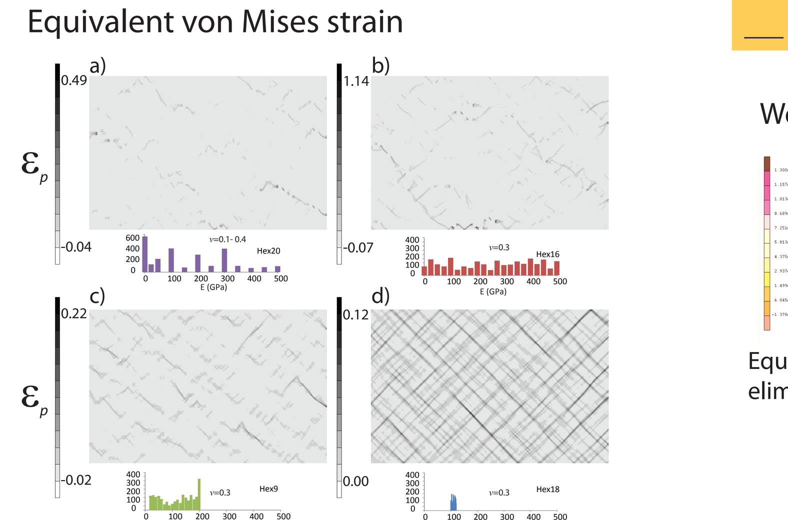

Patterns in equivalent plastic strain. Dark shades are higher values and light shades are lower values of equivalent plastic strain. Models as shown at a strain increment between 0.2-0.5% global strain beyond initial yielding. a) hex20, b) hex16, c) hex9 and d) hex18.

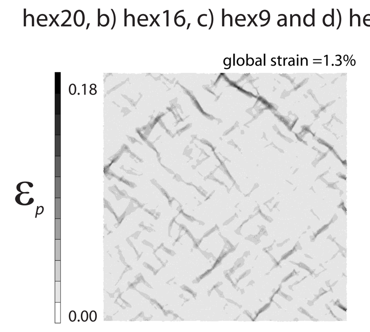

Despite significant differences in the model, including variations in grain shape and size, and the use of the full elastic tensor, a similar pattern of shear localization occurs in the "Barre Granite" model.

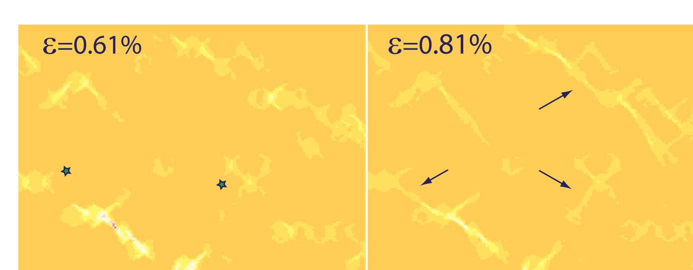

Equivalent plastic strain for a portion of model hex9. Scale bar is equivalent to the width of two grains. At low strain most grains exhibit no plastic strain. Grains where yielding initiates (lighter yellows) develop "fins" that extend outwards at 45 degrees (stars). Fins connect between grains when yielding grains are sufficiently close (arrows).

Work hardening rate (GPa/ε%)

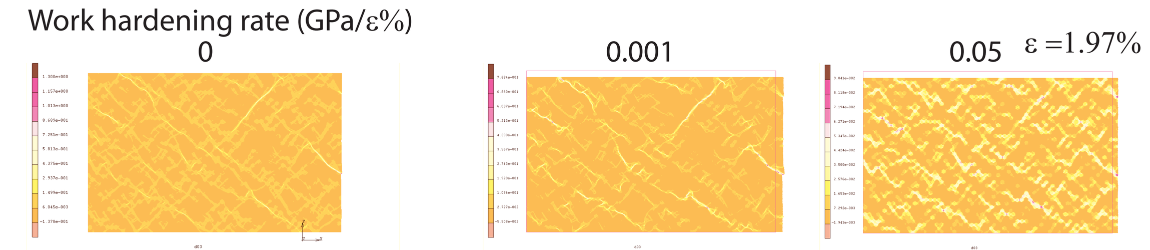

Equivalent plastic strain for model hex9. Including work hardening in the model moderates, but does not eliminate shear localization.

Effect of yeild strength variations of shear localization

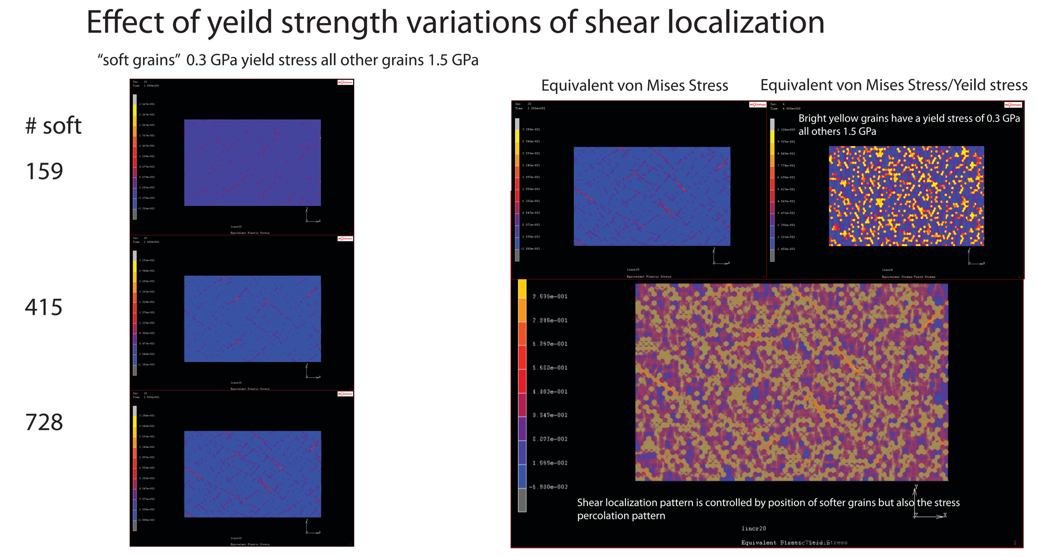

Connections

Stress percolation causes shear localization in granular materials

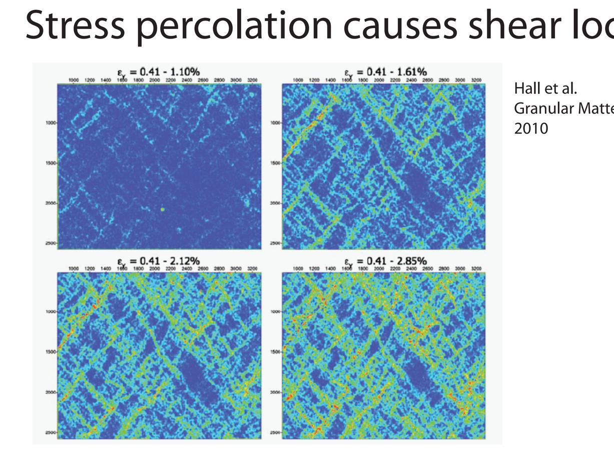

Cummulative internal shear strains in a 2D granular material (rods)
Visualized with digital image correlation

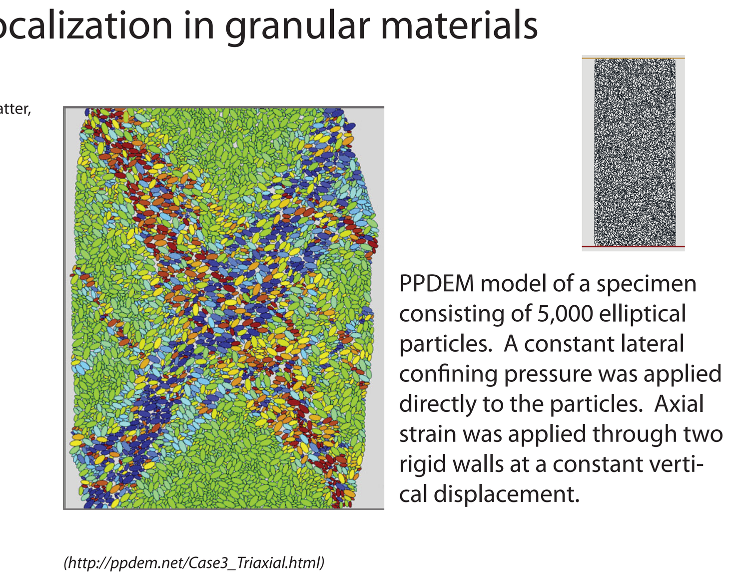

PPDEM model of a specimen consisting of 5,000 elliptical particles. A constant lateral confining pressure was applied directly to the particles. Axial strain was applied through two rigid walls at a constant vertical displacement.

Shear localization is observed during ductile deformation in fully dense polycrystalline materials

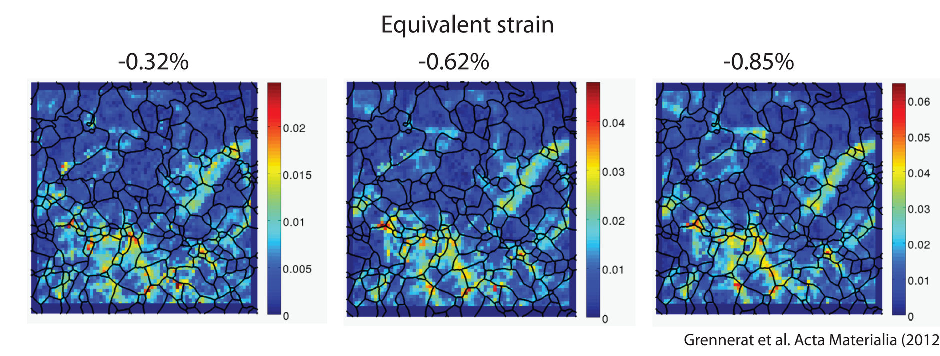

Plain strain deformation of columnar ice visualized with digital image correlation. Local strain can be 10 times the macroscopic strain. The shear band width is smaller than the grain size and grain strain does not correlate with the Schmid factor. Local tensile stresses are also observed.

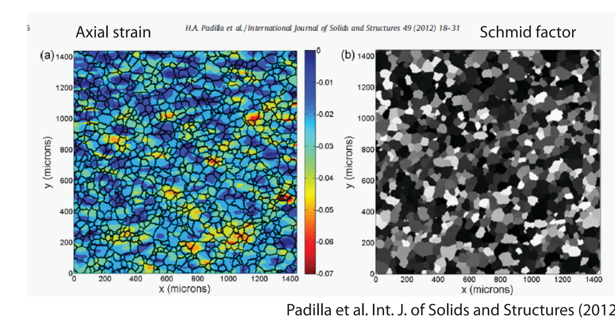

Cross-rolled zirconium under uniaxial compression imaged with digital image correlation. No correlation between local strain and Schmid factor is observed. Shear localization occurs in bands at 45 to compression.

Shear localization result from hetereogeneity in ductile rheology in models of viscous deformation

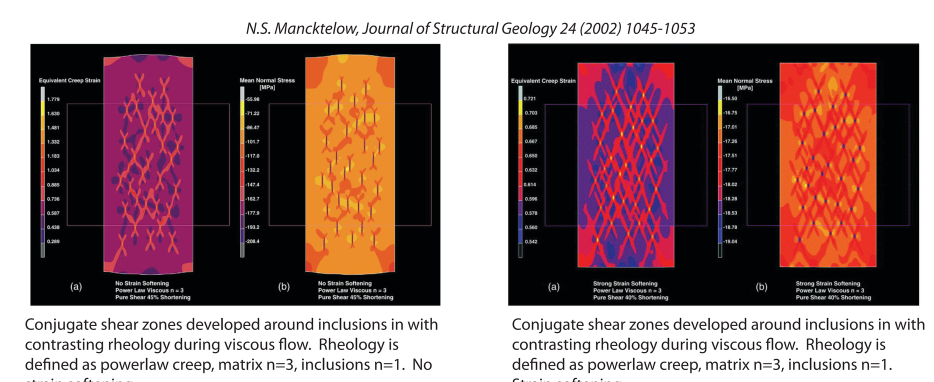

Conjugate shear zones developed around inclusions in with contrasting rheology during viscous flow. Rheology is defined as powerlaw creep, matrix n=3, inclusions n=1. No strain softening

Conjugate shear zones developed around inclusions in with contrasting rheology during viscous flow. Rheology is defined as powerlaw creep, matrix n=3, inclusions n=1. Strain softening

Implications of Stress Percolation

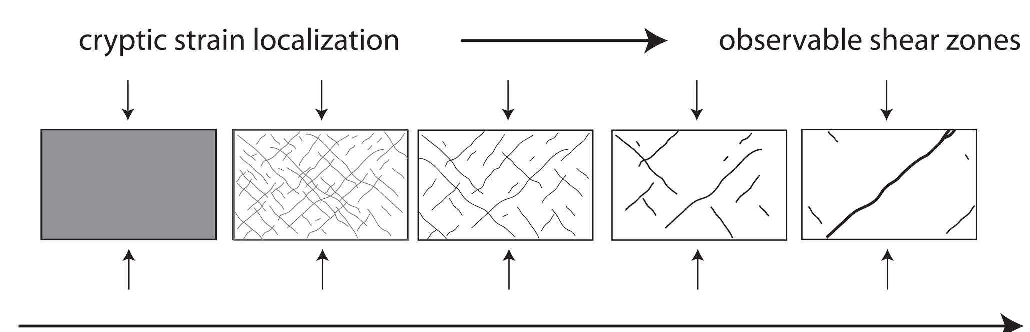

Component Heterogeneity

All polycrystalline rocks will experience some level of shear localization during ductile deformation
- monomineralic rocks will
  - tend to produce cryptic localization
  - level of strain is modulated on the grain scale
  - deformation appears distributed on the macroscopic scale
- polyphase rocks will
  - be more likely to produce large scale shear zones

Pre-existing weakness is not required to produce ductile shear zones

For experimentalists - minimum sample size (representative volume element) for experiments:
- may be larger than anticipated
- will not be the same for all materials

This research was supported by DOE NNSA Cooperative Agreement No. DE FC52-06NA26274 and partially supported by National Science Foundation grant EAR07-41521.

Grennerat F. et al., Experimental characterization of the intragranular strain field in columnar ice during transient creep. Acta Mater. 60, 3655–3666 (2012)
Hall S.A, · MuirWood D , Ibraim ·E. and Viggiani G Localised deformation patterning in 2D granular materials revealed by digital image correlation. Granular Matter (2010) 12:1–14, DOI 10.1007/s10035-009-0155-1
Padilla H.A., Lambros J., Beaudoin A.J., Robertson I.M., Relating inhomogeneous deformation to local texture in zirconium through grain-scale digital image correlation strain mapping experiments. Int. J. Solids and Struct. 49, 18–31 (2012)